Zoomorphology (2024) 143:231–248
https://doi.org/10.1007/s00435-024-00642-x

RESEARCH

# Anatomical and morphometric studies on the axial skeleton of ostrich (*Struthio camelus*)

**Menna Allah M. Kassem**[1] · **Reem R. Tahon**[1] · **Medhat A. El-Ayat**[1]

Received: 24 December 2023 / Revised: 7 January 2024 / Accepted: 8 January 2024 / Published online: 9 February 2024


## Abstract

The present study showed a descriptive anatomical study of the parts of the axial skeleton in the ostrich *(Struthio camelus)* in addition to a morphometric study of each bone. We studied 7 male ostriches aged from 1 to 3 years with an average weight of 120.00 kg. The cranium exhibited two vast orbits supported by a sclerotic ring. Hyoid apparatus was fine delicate horseshoe-shaped and comprised *Basihyale*, *Urohyale*, and *Cornu branchiale*. *Cornu branchiale* were paired and long rod-shaped, consisting of a proximal bony part *Ceratobranchiale* and slightly curved distal cartilaginous process, the *Epibranchiale* located on either side of the hyoid apparatus. The whole vertebral column comprised 54 vertebrae, including 18 cervical vertebrae, 7 separated thoracic vertebrae, a *synsacrum*, and 9 separated caudal vertebrae. Atlas had a butterfly-shape with a narrow width and large vertebral foramen. Axis had a protruded dens with a rounded tip that arose from the cranial surface of the body for articulation with the *Incisura fossae* of atlas. Several *Pneumatic foramina* were found in the cervical vertebrae. The transverse foramen was found in all the cervical vertebrae except atlas. The ribs were nine pairs in number, the sternal ribs extended from the third to the seventh rib while the rest were asternal floating ribs. The sternum was a broad quadrilateral extensive bone, lacking the keel bone. It had dorsally several *Pneumatic foramina*.

**Keywords** Axial skeleton · Mandible · Male ostrich · Pygostyle · Skull · Sternum · *Synsacrum* · Vertebrae

## Abbreviations

| | |
|---|---|
| OO | *Os occipital* |
| OS | *Os sphenoidale* |
| OSQ | *Os squamosum* |
| OP | *Os parietale* |
| OF | *Os frontale* |
| *ON* | *Os nasale* |
| *OL* | *Os lacrimale* |
| *OPM* | *Os premaxillare* |
| *OM* | *Os maxillare* |
| *OJ* | *Os jugale* |
| *OPA* | Os *palatinum* |
| *OPT* | *Os pterygoideum* |
| OQ | *Os quadratum* |
| OA | *Os articulare* |
| C | Cervical vertebra |
| C1 | Atlas |
| C2 | Axis |
| C9 | Ninth cervical vertebra |
| C17 | Seventeenth cervical vertebra |
| C18 | Last cervical vertebra |
| T | Thoracic vertebra |
| R1 | First rib |
| R2 | Second rib |
| R3 | Third rib |
| R4 | Fourth rib |
| R5 | Fifth rib |
| R6 | Sixth rib |
| R7 | Seventh rib |
| R8 | Eighth rib |
| R9 | Ninth rib |

## Background

Ostrich (*Struthio camelus*) is a ratite bird that belongs to the family *Struthionidae* and the genus *Struthio* (Kummrow 2015). It was mentioned in fossils that the origin of *Struthio* is African in origin and was seen in African Namibia hundreds of years ago (Mikhailov and Zelenkov 2020). Recent developments in ostrich farming have increased the demand

✉ Reem R. Tahon
Reemtahon@cu.edu.eg

[1] Anatomy and Embryology Department, Faculty of Veterinary Medicine, Cairo University, Giza, Egypt

for knowledge concerning this bird (Deeming 1999). The ostrich is a member of the *Struthioidae* family, genus *Struthio*, and species *Struthio camelus* (Moselhy et al. 2018). The ostrich has four subspecies: the North African ostrich (*Struthio camelus camelus*), the Somali ostrich (*Struthio camelus molybdophanes*), the Massai ostrich (*Struthio massaicus*), and the South African ostrich (*Struthio australis*) (Kummrow 2015). The ostrich is the largest living bird, reaching up to 2.75 m in height and weighing up to 150 kg (Deeming 1999). Ostrich has great economic worth, especially in the production of meat of high value in terms of quantity and quality as well as high quality of feathers and leather (Moselhy et al. 2018).

The ostrich skeleton consisted of axial and appendicular skeleton (Kassem et al. 2023). The axial skeleton is comprised of the cranium, sclerotic ring, mandible, hyoid bone, vertebral column, ribs, and sternum (Kassem et al. 2023). The cranium was bulbous and the face was pyramidal (Dyce et al. 2009). The sclerotic ring found that there was a ring of small bony plates around the eye pupil in all birds, it protected their eyes from extreme distortion (Kaiser 2010). The vertebral column was formed from 56 (range of 54–57) vertebrae in the ostrich (Deeming 1999). The sternum in flightless birds (ostrich, Emu and rhea) lacked the sternal keel as the sternum flattened (Feneck et al. 2021). All ratites had a broad smooth, bowl-shaped sternum without a keel (Brett and Hopkins 1991).

Searching in the scientific journals and periodicals that dealt with the anatomy of the skeleton in ostriches, it was found scarce and incomplete. The main goal of the current study is to perform a complete descriptive anatomical study of the various components of the axial skeleton in the ostrich.

## Results

The ostrich skull consisted of the cranium, sclerotic ring, mandible (Fig. 1a), and hyoid apparatus**.** The skull was rhombus shaped in outline dorsally. It had an extremely large orbit supported by a sclerotic ring. The cranium had two parts; the neurocranium caudally occupied by the brain and the splanchnocranium composed of the facial bones. The Neurocranium consisted of *os occipital* (OO)*, os sphenoidale* (OS), *os squamosum* (OSQ)*, os parietale* (OP)*, and os frontale* (OF). The splanchnocranium consisted of vomer bone and *os ethmoidale* (single bones), *os nasale (ON), os lacrimale (OL), os premaxillare (OPM), os maxillare (OM), os jugale (OJ), os palatinum (OPA)*, *os pterygoideum (OPT)* and *os quadratum (OQ)* (paired bones). In ostrich, several pneumatic bones were found in the skull including vomer, pterygoid, basisphenoid, squamosal, and parietal bones. Orbit diameter was 5.00 ± 0.11 cm between the cranial and caudal bony edges of the orbit. The metric data of the skull is shown in (Table 1).

The neurocranium; The occipital bone *(Os occipitale)* (OO) was composed of three parts around the *foramen magnum*; *Os basioccipitale, Os exoccipitale and Os supraoccipitale*. *Os basioccipitale* had a semicircular single occipital condyle (*condyles occipitalis*) with an *Incisura mediana condyli* in the middle caudally (Fig. 2b). *Os exoccipitale* were paired bones with large, protruded *processus exoccipitalis (processus paroccipitalis)* on both sides of the *foramen magnum* (*Foramen occipital magnum*) laterally (Fig. 2b). *Os supraoccipitale* was the caudal part of the occipital bone, carrying *crista nuchalis sagittalis* and the arched *crista nuchalis transversa* (Fig. 2a).

The Sphenoid bone *(Os sphenoidale)* laid on the floor of the cranial cavity, rostral to basioccipital bone. It consisted of *Os basisphenoidale* caudally; *Os parasphenoidale* (*Rostrum parasphenoidalis*) rostrally; and *Os laterosphenoidale* laterally. *Os basisphenoidale* was composed of a body and two temporal wings laterally (Fig. 2b, c). The *Os parasphenoidale* consisted of a median body and two rod-like parasphenoid wings (*Ala parasphenoidalis*) articulating with pterygoid bone (Fig. 2c). *Os laterosphenoidale* were two lateral orbital wings at caudal wall of orbit that diverged from the interorbital septum caudolaterally (Fig. 4a).

The Parietal bone (*Os parietale)* formed the caudodorsal part of the cranial cavity. It was curved and bulged caudally between the supraoccipital bone and frontal bone. It had a parietofrontal suture related to frontal bone rostrally (Fig. 3a). The Frontal bone (*Os frontale*) was a large bone with the greatest height of the skull at the frontal elevation. It had lacrimal process (Fig. 3a), postorbital processes (Fig. 4a) and the orbital wing of frontal bone (Fig. 4a) at the caudomedial part of the orbit. *Fossa glandulae nasalis* was a depression on the dorsal aspect of the supraorbital margin that was occupied by the salt gland leading to the Supraorbital fissure (Fig. 3c).

The squamosal bone *(Os squamosum)* was located at the caudolateral part of the cranium between the parietal, frontal and laterosphenoid bones. It had a broad zygomatic process (*processus zygomaticus*) (Fig. 4a), directed rostroventrally, caudal to the temporal fossa (*fossa temporalis*), and lateral to the quadrate bone. *Ossa otica* or otic bone was highly pneumatic, articulated to *process oticus* of quadrate bone by an articular groove (Fig. 2b).

The splanchnocranium; the ethmoid bone (*Os ethmoidale*) consisted of *Os mesethmoidale* and *Os ectoethmoidale*. The *Os mesethmoidale* formed most of the interorbital septum rostrally (Fig. 4a), it formed *lamina dorsalis* which was a transverse plate perpendicular to interorbital septum (Fig. 3a). *Os ectoethmoidale* formed the rostral wall of the orbit rostrally to separate it from the nasal cavity.

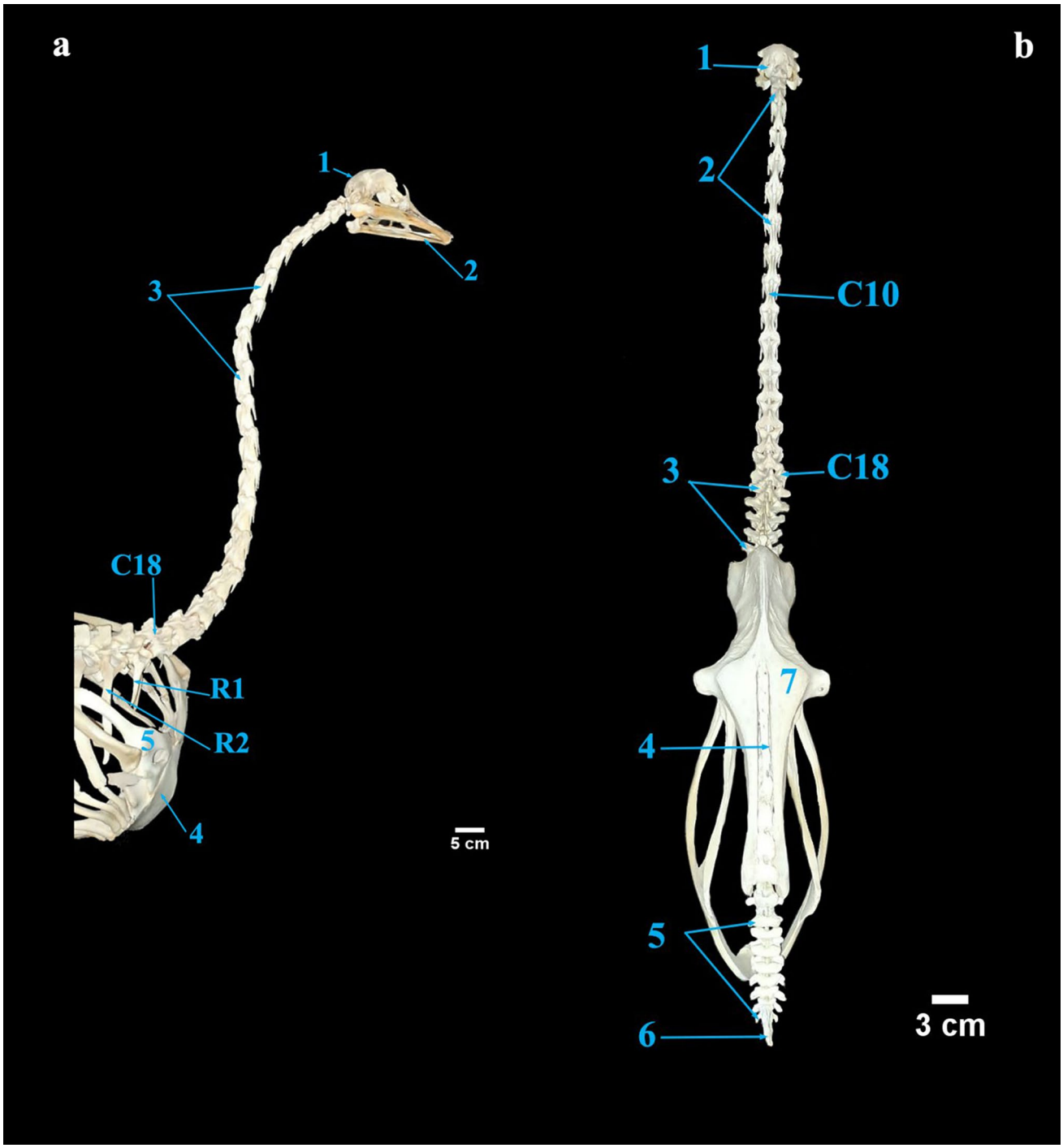


**Fig. 1** **a** Lateral view of ostrich skull with the cervical vertebrae connected to thoracic cage. 1 Cranium. 2 Mandible. 3 Cervical vertebrae. 4 Sternum. 5 Scapulocoracoid. C18 Eighteenth cervical vertebra. R1 First rib. R2 Second rib. **b** Ostrich vertebral column mounted in situ and articulated with Os coxae. 1 Skull. 2 Cervical vertebrae. C10 Tenth cervical vertebra. C18 Last cervical vertebra. 3 Thoracic vertebrae. 4 Synsacrum. 5 Free Caudal vertebrae. 6 Pygostyle

The interorbital septum was extended from the orbital wing of *os frontale*, o*s mesethmoidale* and *os laterosphenoidale*. It was perforated by a large single optic foramen and an ophthalmic foramen. On its caudoventral part, it also had the maxillomandibular foramen dorsal to quadrate bone. It had a *Fonticuli orbitocraniales* between the orbital wing of frontal bone and mesethmoidal bone caudally (Fig. 3b).

**Table 1** Showing the metric data of the skull of ostrich (*Struthio camelus*)

| | Length (cm) | Width (cm) |
|---|---|---|
| Cranium | 20.00 ± 1.09 | 9.00 ± 0.46 |
| Mandible | 16.50 ± 0.28 | 9.00 ± 0.69 |

The vomer bone was a single median long and laterally compressed (slightly) wide tube. Its body fused caudally to the parasphenoid bone, and its process articulated laterally to pterygoid bone and rostrally to palatine bones (Fig. 2c).

The Nasal bones (*Os nasale*) formed the roof and lateral boundary of the nasal cavity, a small part of the upper beak and the dorsal boundary of the *Aperatura nasi ossea* (Fig. 3a). Its processes were *processus frontalis*, *processus lateralis nasalis*, and *processus premaxillare*. *Processus frontalis* of ON formed the nasofrontal hinge as it

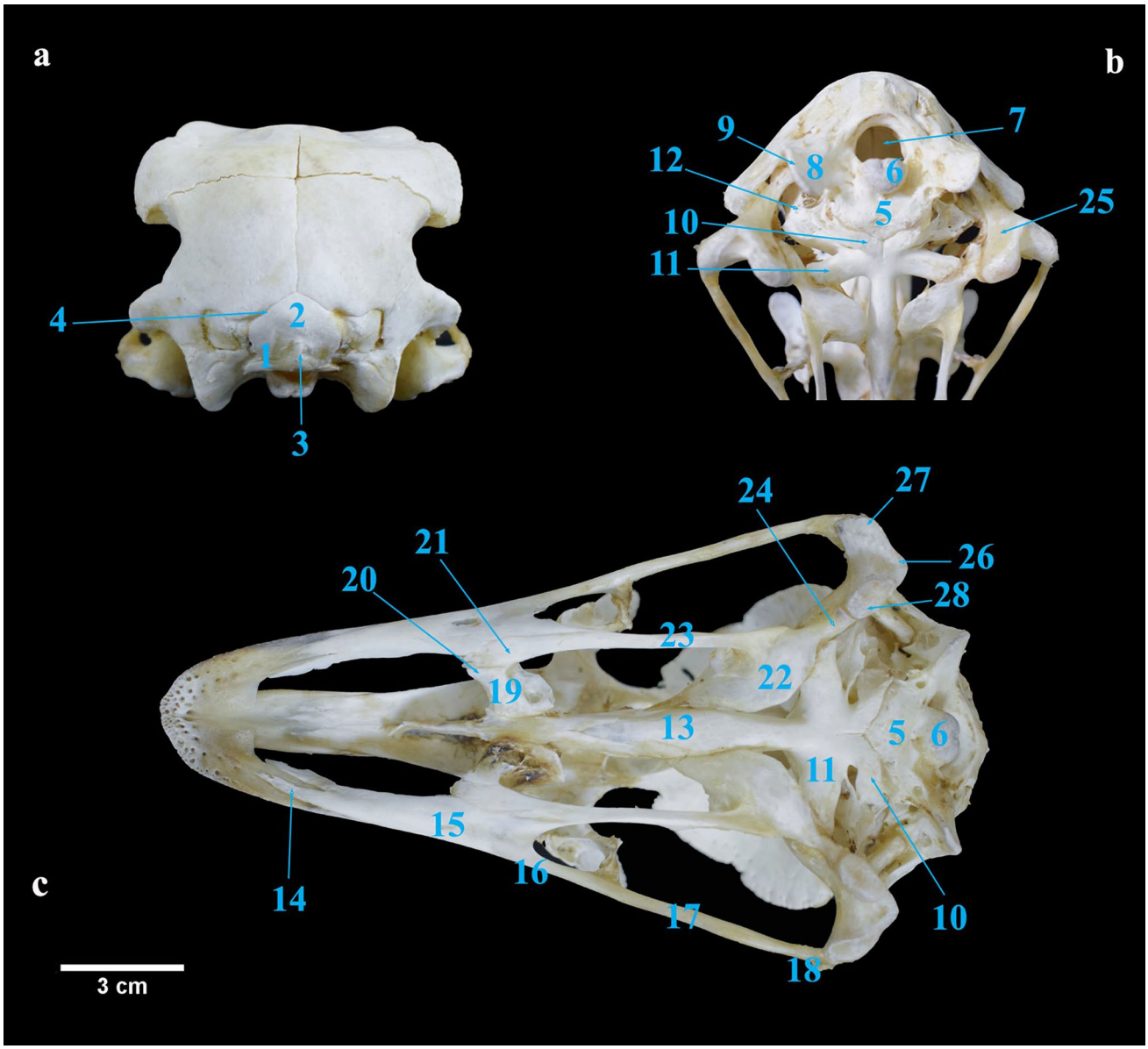


**Fig. 2** **a–c** Caudal, Caudoventral and Ventral views of Ostrich Cranium. 1 *Os occipitale* (OO). 2 *Os supraoccipitale*. 3 *Crista nuchalis sagittalis*. 4 *Crista nuchalis transversa*. 5 *Os basioccipitale*. 6 *Condyles occipitalis*. 7 Foramen magnum. 8 *Os exoccipitale*. 9 *Processus exoccipitlis* (*processus paroccipitalis).* 10 *Os basisphenoidale*. 11 *Ala parasphenoidalis*. 12 *Ossa otica*. 13 Vomer bone. 14 *Processus premaxillaris* of OM. 15 *Os maxillare (OM)*. 16 *Processus jugalis* of OM. 17 *Os jugale*. 18 *Os quadratojugale*. 19 *Os palatinum* (OP). 20 *Processus maxillaris* of OP. 21 *Processus pterygoideus* of OP. 22 *Os pterygoideum* (OPT). 23 *Pars palatina* of OPT. 24 *Processus quadraticus* of OPT. 25 *Os quadratum* (OQ). 26 *Condyles caudalis.* 27 *Condyles lateralis.* 28 *Condyles medialis*

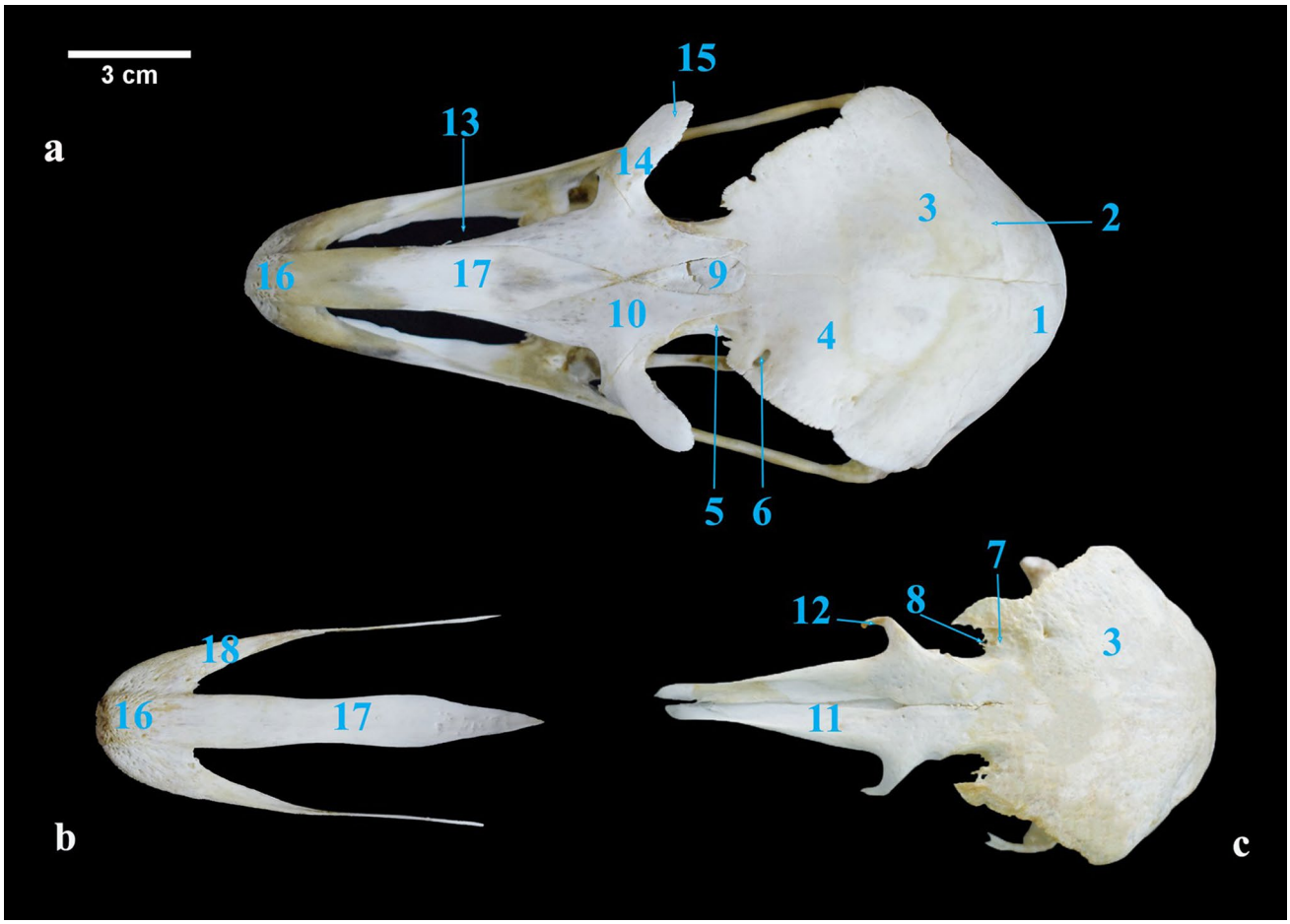


**Fig. 3** **a** Dorsal view of ostrich cranium, **b** separated premaxillary bone, **c** ostrich cranium without the premaxillary, lacrimal and jugal bones. 1 *Os parietale*. 2 Parieto-frontal suture. 3 *Os frontale* (OF). 4 *Facies orbitalis* of OS. 5 *Processus lacrimalis* of OS. 6 Supraorbital foramen. 7 *Fossa glandulae nasalis.* 8 Supraorbital fissure. 9 *Lamina dorsalis of os mesethmoidale*. 10 *Os nasale* (ON). 11 *Processus premaxillaris* of ON. 12 Lateral nasal process. 13 *Aperatura nasi ossea.* 14 *Os lacrimale* (OL). 15 Lacrimal process. 16 Os premaxillare (OPM). 17 *Processus frontalis* of OPM. 18 *Processus maxillaris* of OPM

articulated with the frontal bone rostrally. *Processus premaxillare* of ON (Fig. 3c) articulated dorsally with premaxillary bone (*processus frontalis*) (Fig. 3b). The lateral nasal process articulated laterally with the lacrimal bone.

Lacrimal bones (*Os lacrimale*) were wide comma shape bones forming the rostral boundary of the orbit. They had caudally placed frontal process, caudolaterally placed lacrimal process (Fig. 3a), and caudoventrally placed bifid jugal processes (Fig. 4a, c) to join the jugal bone and were related to the *Os ectethmoidale* (Fig. 4a).

Premaxillary bones (*Os premaxillare*) formed the *rostrum maxillae* of the upper beak by the fusion of right and left bones (Fig. 3a). *Rostrum maxillae* had numerous *Foramina* neurovascularia. *Processus frontalis* of OPM articulated with the nasal and frontal bones (Fig. 3a). *Processus maxillaris* of OPM arose laterally from the *rostrum maxillae* and connected to the maxilla with its narrow ends (Fig. 3b).

Maxillary bones *(Os maxillare)* formed most of the ventral rim of upper beak and a part of the osseous part of hard palate (Fig. 2c). *Processus premaxillaris* of OM was connected to the premaxillary bone. *Processus jugalis* of OM articulated with the jugal bone.

Jugal bones (*Os jugale*) were thin rod-like bones which were the most ventral bone of the orbit placed caudal to the upper beak (Fig. 2c). The jugal arch (*arcus jugalis*) was formed of fused *Processus jugalis* of OM (Fig. 2c), *Os jugale* and *Os quadratojugale* (Fig. 4a).

Palatine bones (*Os palatinum*) were quadrilateral plates constituting the bony roof of pharynx (Fig. 2c). *Processus maxillaris* of OP connected to maxillary bone rostro-laterally. *Processus pterygoideus* of OP arose caudolaterally to the rostral pterygoid bone.

Pterygoid bones *(Os pterygoideum)* were pear-shaped bones placed on both sides of the root vomer bone (Fig. 2c). *Pars palatina* of OPT articulated rostrally with the palatine

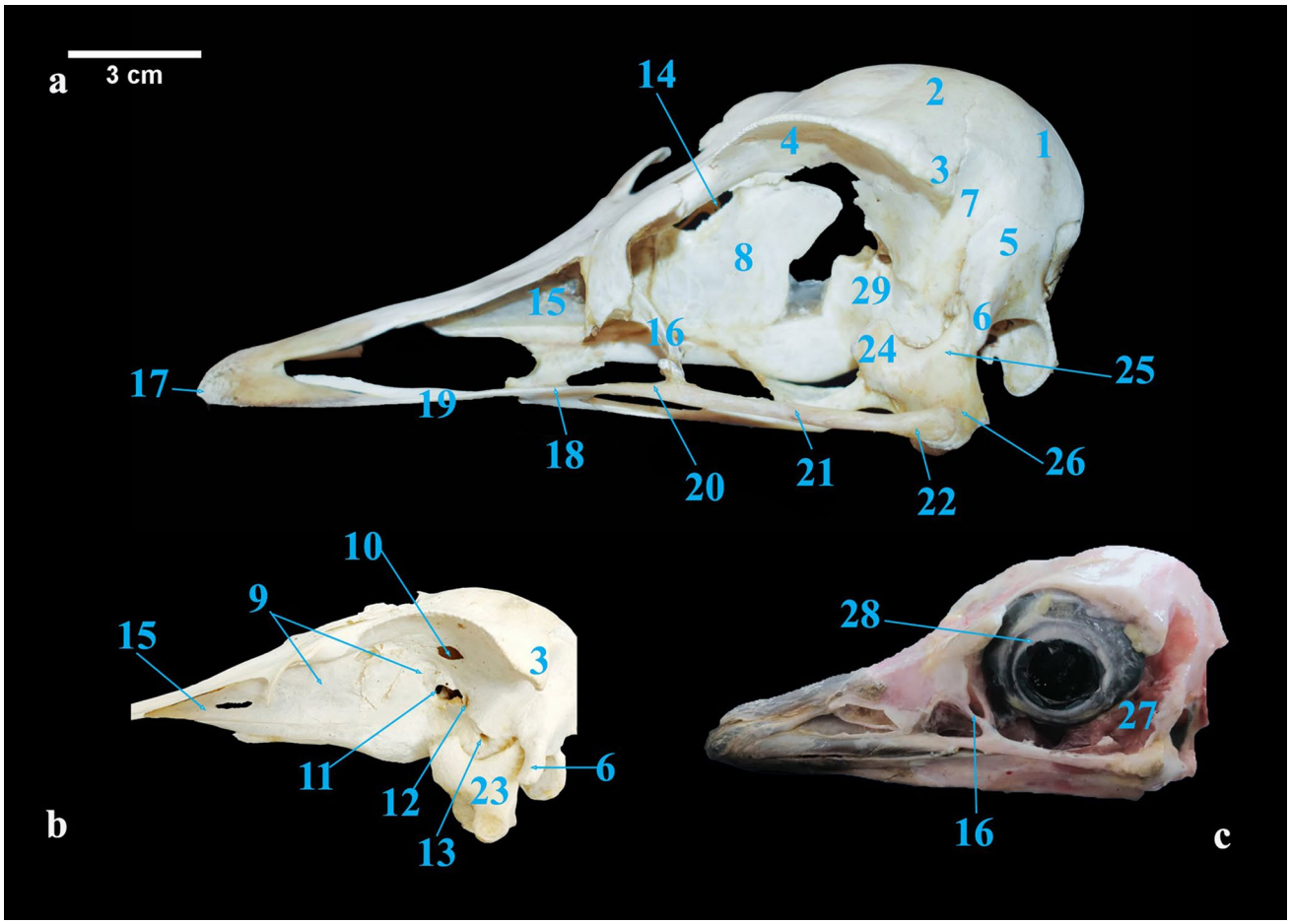


**Fig. 4** **a**, **b** Left lateral views of ostrich cranium of 1 year age and 2.5 years respectively, **c** left lateral view of ostrich head. 1 *Os parietale*. 2 *Os frontale*. 3 Postorbital processes. 4 Orbital wing of OF. 5 *Os squamosum*. 6 *Processus zygomaticus*. 7 *Fossa temporalis*. 8 *Os mesethmoidale*. 9 Interorbital septum. 10 *Fonticuli orbitocraniales*. 11 Single optic foramen. 12 Ophthalmic foramen. 13 Maxillomandibular foramen. 14 Orbitonasal foramen. 15 Internasal septum. 16 Jugal process of OL. 17 *Rostrum maxillae*. 18 *Os maxillare* (OM). 19 *Processus premaxillaris* of OM. 20 *Processus jugalis* of OM. 21 Jugal bone. 22 Quadratojugal bone. 23 *Os quadratum* (OQ) 24 *Processus orbitalis* of OQ. 25 *Processus oticus* of OQ. 26 *Processus mandibularis* of OQ. 27 Orbit. 28 Sclerotic ring. 29 *Os Laterosphenoidale*

bones. *Processus quadraticus* of OPT was short and connected to the medial condyle of the mandibular process of quadrate bone.

Quadrate bones *(Os quadratum)* were irregular quadrilaterals, connecting the upper beak bones to the neurocranium (Fig. 4b). *Processus mandibularis* of OQ (Fig. 4a) was the ventral boundary of quadrate carrying *condyles caudalis, condyles lateralis* and *condyles medialis* (Fig. 2c) to articulate with the lateral, medial and caudal facets of the articular bone of mandible (Fig. 5b). Also, the *Processus mandibularis* articulated medially with pterygoid bone by *condyles pterygoideus* and laterally with the quadratojugal bone. *Processus orbitalis* formed the dorsorostral angle of quadrate, articulating with the laterosphenoid medially (Fig. 4a). *Processus oticus* directed dorsocaudally articulating with *process zygomaticus* (Fig. 4a). The sclerotic ring was a ring of small bony plates within the eye sclera (Fig. 4c).

The Mandible *(Ossa mandibulae)* was V-shaped with slightly curved right and left mandibular rami (*Ramus mandibulae*) fusing rostrally to form the mandibular symphysis (*symphysis mandibulae*) as the apical part of the mandible (Fig. 5a). *Ossa mandibulae* was constituted of seven bones: *Os mentomandibulare*, *Os dentale*, *Os spleniale*, *Os supra-angulare*, *Os prearticulare*, *Os articulare*, and *Os angulare*. They were fused to each other in the adult by ossification except the suture between angular and supra-angular is not completely ossified.

The paired *Os mentomandibulare* fused forming the *rostrum mandibulae* (Fig. 5a) and carrying several mandibular neurovascular openings and rostral mandibular foramen medially (Fig. 5b). *Os dentale* formed most of the ramus rostrally after the first part (Fig. 5a). *Os spleniale* carried a narrow mylohyoid line (Fig. 5b) medially. *Os supra-angulare* had the coronoid process dorsally and the caudal mandibular

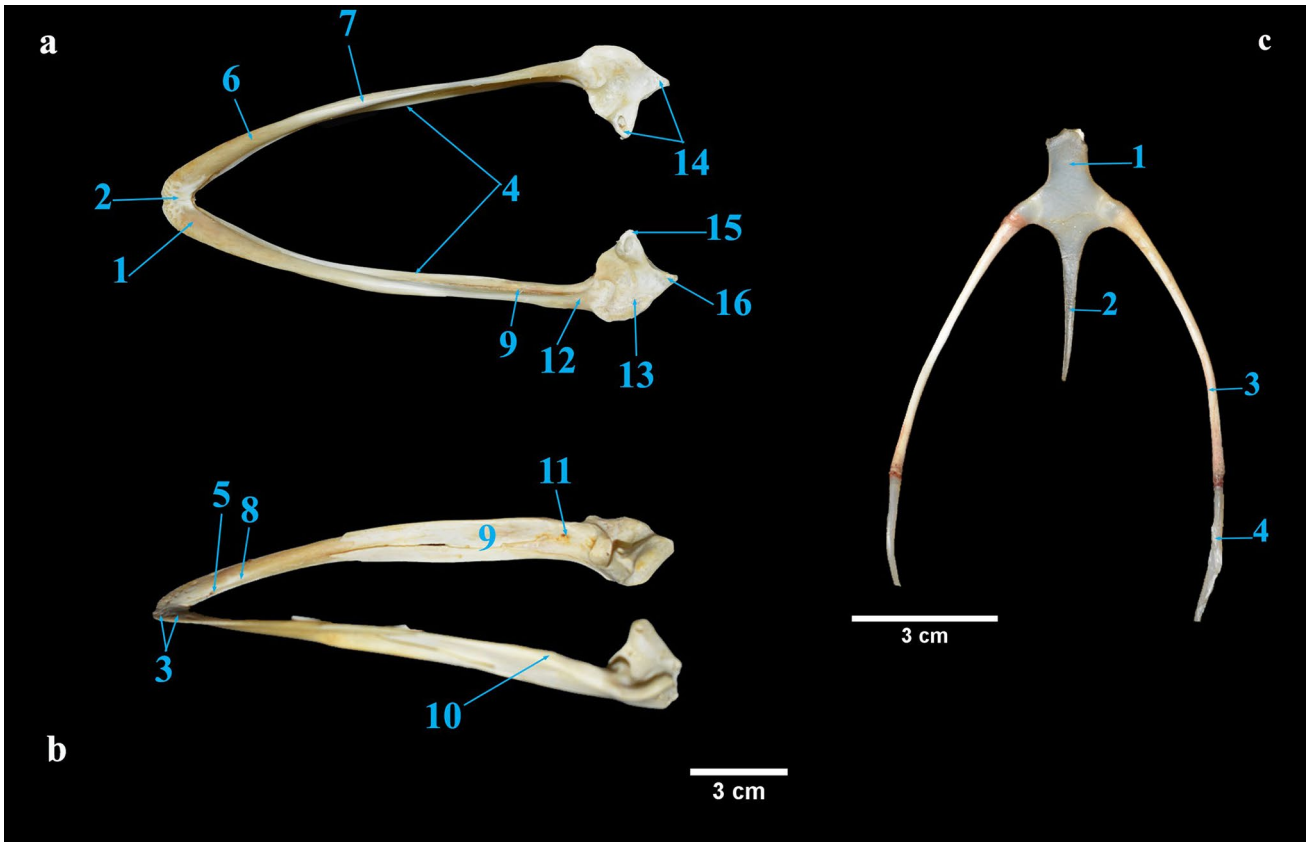


**Fig. 5** **a**, **b** Dorsal and lateral views of ostrich *ossa mandibulae*. 1 *Os mentomandibulare*. 2 *Rostrum mandibulae*. 3 *Fenestrae neurovascularia mandibulae*. 4 *Rami Mandibulae*. 5 *Foramen mandibulae rostralis*. 6 *Os dentale*. 7 *Os spleniale*. 8 *Mylohyoidus line*. 9 *Os supra-angulare*. 10 *processus coronoideus*. 11 *Foramen mandibulae caudalis*. 12 *Os prearticulare*. 13 *Os articulare*. 14 *Os angulare*. 15 *Process medialis mandibulae*. 16 *Process lateralis mandibulae*. **c** Hyoid apparatus (*Apparatus hyobranchialis*) of Ostrich. 1 *Basihyale* (*Basibranchiale rostrale*). 2 Urohyale (*Basibranchiale caudale*). 3 *Ceratobranchiale*. 4 *Epibranchiale*

foramen medially (Fig. 5b). *Os prearticulare* was a small bone placed more caudally (Fig. 5a). *Os articulare* articulated by its articular surface (*cotyla caudalis, cotyla lateralis and cotyla medialis)* forming the quadratomandibular joint. *Os angulare* was the last caudal one, with two short processes: *processus medialis mandibulae* and *processus lateralis mandibulae* (Fig. 5a).

The hyoid apparatus (*Apparatus hyobranchialis*) was a fine delicate horseshoe-shaped solitary apparatus, located in the midline of the cervical region rostrally at the base of the mandible and caudally at the third cervical vertebra. It was comprised of three parts: *Basihyale* (*Basibranchiale rostrale*), Urohyale (*Basibranchiale caudale*), and hyoid rami (*Cornu branchiale*). *Basihyale* was a median unpaired bony element of the hyoid apparatus, it articulated caudally with the urohyale, while laterally with the hyoid rami. *Urohyale* was an ossified bony part of hyoid, caudal to *basihyale* that articulated with the hyoid rami laterally. Hyoid rami were paired and long rod-shaped, consisted of a proximal bony part *Ceratobranchiale* and slightly curved distal cartilaginous process, the *Epibranchiale* located on either side of the hyoid apparatus and were articulated with the *basihyale* and *urohyale* rostrally, while their caudal ends were free (Fig. 5c).

The vertebral column (*columna vertebralis*) comprised in ostrich 54 vertebrae, including eighteen cervical vertebrae, seven separated thoracic vertebrae, *synsacrum*, and nine separated caudal vertebrae (Fig. 1b). The *synsacrum* was comprised of twenty vertebrae: the fused last two thoracic, seven lumbar, five sacral and six caudal vertebrae.

The Cervical vertebrae were composed of 18 vertebrae, arranged in three series; the cranial series from C3 to C10, the middle one from C11 to C16, while the caudal series were C17 and C18 (Fig. 6a). Atlas (first cervical vertebra) was a butterfly in shape with a narrow width and large vertebral foramen (Fig. 6b, c). For anatomical description, it had *corpus atlantis*, dorsal and ventral arches, and cranial and caudal surfaces. The *corpus atlantis* occupied the *Condyloid fossa* on its cranial surface for lodging the single occipital condyle of the cranium forming the atlantooccipital joint (Fig. 6b). The caudal surface of the body had a nearly flat axis articular facet and on the inner surface of the ventral

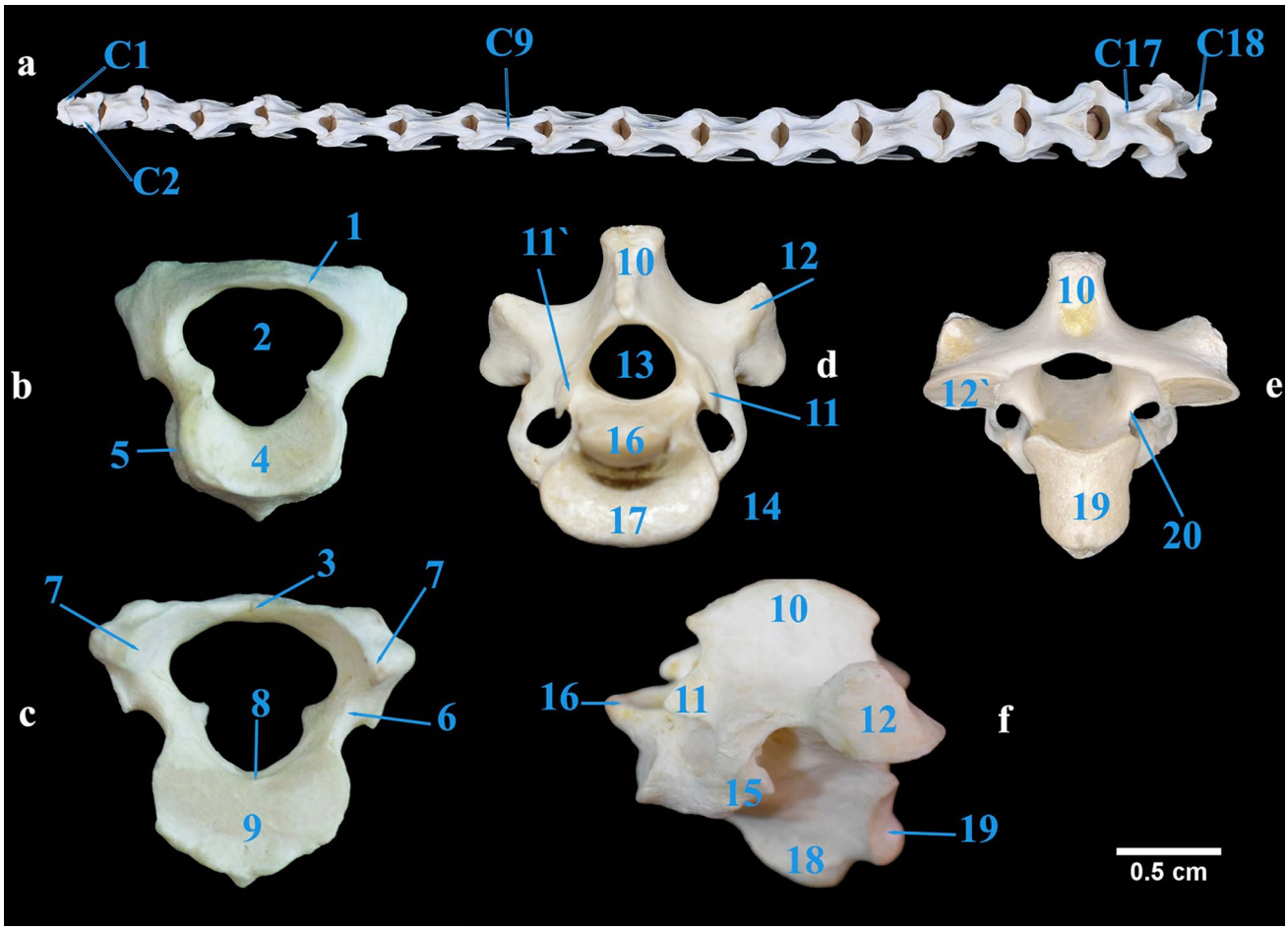


**Fig. 6** **a** Dorsal view cervical vertebrae of Ostrich, **b**, **c** cranial and caudal views of Atlas, **d–f** lateral, cranial and caudal views of Axis. C1 Atlas. C2 Axis. C9 Ninth cervical vertebra. C17 Seventeenth cervical vertebra. C18 Last cervical vertebra. 1 Dorsal arch. 2 Large vertebral foramen. 3 Small notch. 4 Condyloid fossa. 5 *Corpus atlantis*. 6 *Incisura caudalis arcus*). 7 Caudal articular process. 8 *Incisura fossae*. 9 Articular surface of axis. 10 Spinous process of axis. 11 Cranial articular process. 11' Cranial articular facet. 12 Caudal articular process. 12' Caudal articular facet. 13 Vertebral foramen. 14 Transverse foramen. 15 Costal process. 16 Dens (*Odontoid process*). 17 Atlas articular facet. 18 Ventral process of axis. 19 Caudal articular surface. 20 *Incisura arcus caudalis*

arch found the *Incisura fossae* articulated with the dens of the axis (Fig. 6c). The dorsal arch carried a small notch at the midline and the caudal articular processes on both sides caudally which were related ventrally to *Incisura caudalis arcus* (Fig. 6c).

The Axis (second cervical vertebra) (Fig. 6d–f) had a protruded dens (*odontoid process*) with a rounded tip that arose from the cranial surface of the body for articulation with the *Incisura fossae* of atlas (Fig. 6d). On the caudal surface, the body possessed the caudal articular surface (Fig. 6e). A small ventral process (process *ventralis corporis*) projected from the axis body ventrally (Fig. 8f). Two small cranial articular processes were situated dorsolateral to the dens (Fig. 6d), while the Atlas articular surface was just ventral to the dens. A slightly large curved Spinous process (*processus spinosus*) (Fig. 6d) arose from the dorsal arch of axis and was related caudolaterally to the two large caudal articular processes that had oval caudal articular facet directed caudoventrally (Fig. 6e). On the axis arch, a costal process originated and related medially to the transverse foramen (Fig. 6f).

The cranial series of cervical vertebrae had longer bodies and their lengths gradually increased as progressed posteriorly (Fig. 7c). The middle series from C11 to C16 showed the same size (Fig. 7f), while the caudal series showed decreased in length (Fig. 7h, k). The *Ansa costotransversaria* was a small prominence caudal to the cranial articular process forming the lateral wall of the transverse foramen, also the *lamina arcocostalis* extended from *Ansa costotransversaria* ventrally and carried several *pneumatic foramina* in all the cervical series (Fig. 7a). The transverse foramen was found in all the cervical vertebrae except atlas (Fig. 7b, g, i, j). The ventral process was a small ridge on the body placed ventrally, but it was absent

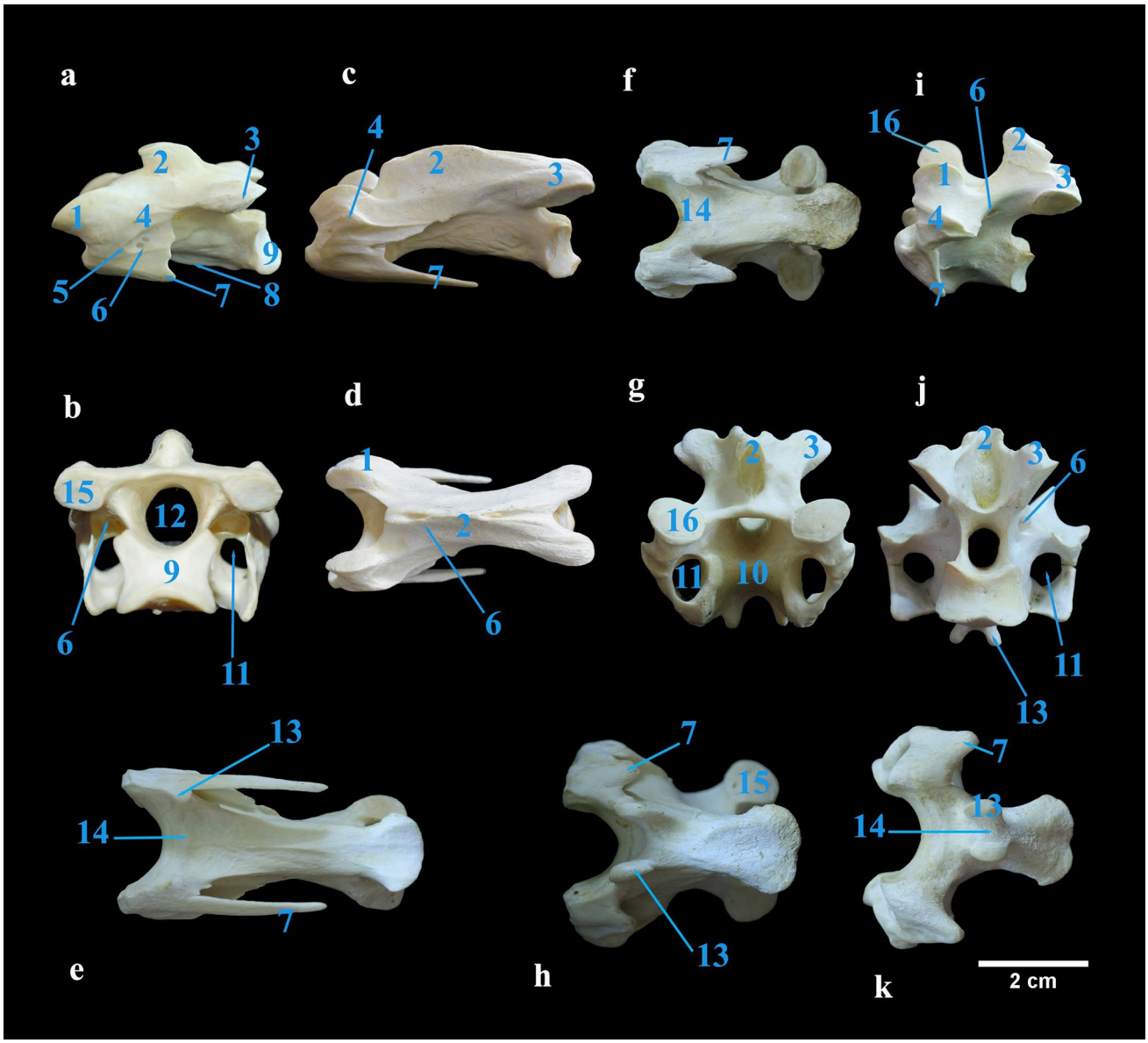


**Fig. 7** **a**, **b** Lateral and caudal views of C3, **c**, **d** lateral and dorsal views of C9**, e**, **f** ventral views of C10 and C16, **g**, **h** cranial and ventral views of C17, **i–k** lateral, caudal, and ventral views of C18 of ostrich. 1 Cranial articular process. 2 Spinous process. 3 Caudal articular process. 4 Ansa costotransversaria. 5 Lamina arcocostalis. 6 Pneumatic foramen. 7 Costal process. 8 Ventral process. 9 Caudal articular surface. 10 Cranial articular surface. 11 Transverse foramen. 12 Vertebral foramen. 13 Carotid process. 14 Carotid sulcus. 15 Caudal articular facet. 16 Cranial articular facet

in the caudal series. The metric data of cervical vertebrae is shown in (Table 2).

The thoracic vertebrae in ostrich were nine in number, comprising the first seven separated vertebrae (Fig. 8) and the last two were fused with the synsacrum (Fig. 9b). All these vertebrae had pneumatic foramina both cranially and caudally. The dorsal spinous processes of the first three vertebrae were short (Fig. 8a, b), small quadrilateral plate which increased sharply in height to be more rectangular in shape (Fig. 8e, g). The length of the thoracic vertebrae increased

**Table 2** Showing the Metric Data of the cervical vertebrae of ostrich (*Struthio camelus*)

| | Length (Cm) | Width (Cm) |
|---|---|---|
| Atlas | 0.40 ± 0.05 | 1.20 ± 0.05 |
| Axis | 3.20 ± 0.11 | 0.80 ± 0.11 |
| Average of 3rd to 18th cervical vertebrae | 6.34 ± 0.22 | 2.76 ± 0.238 |

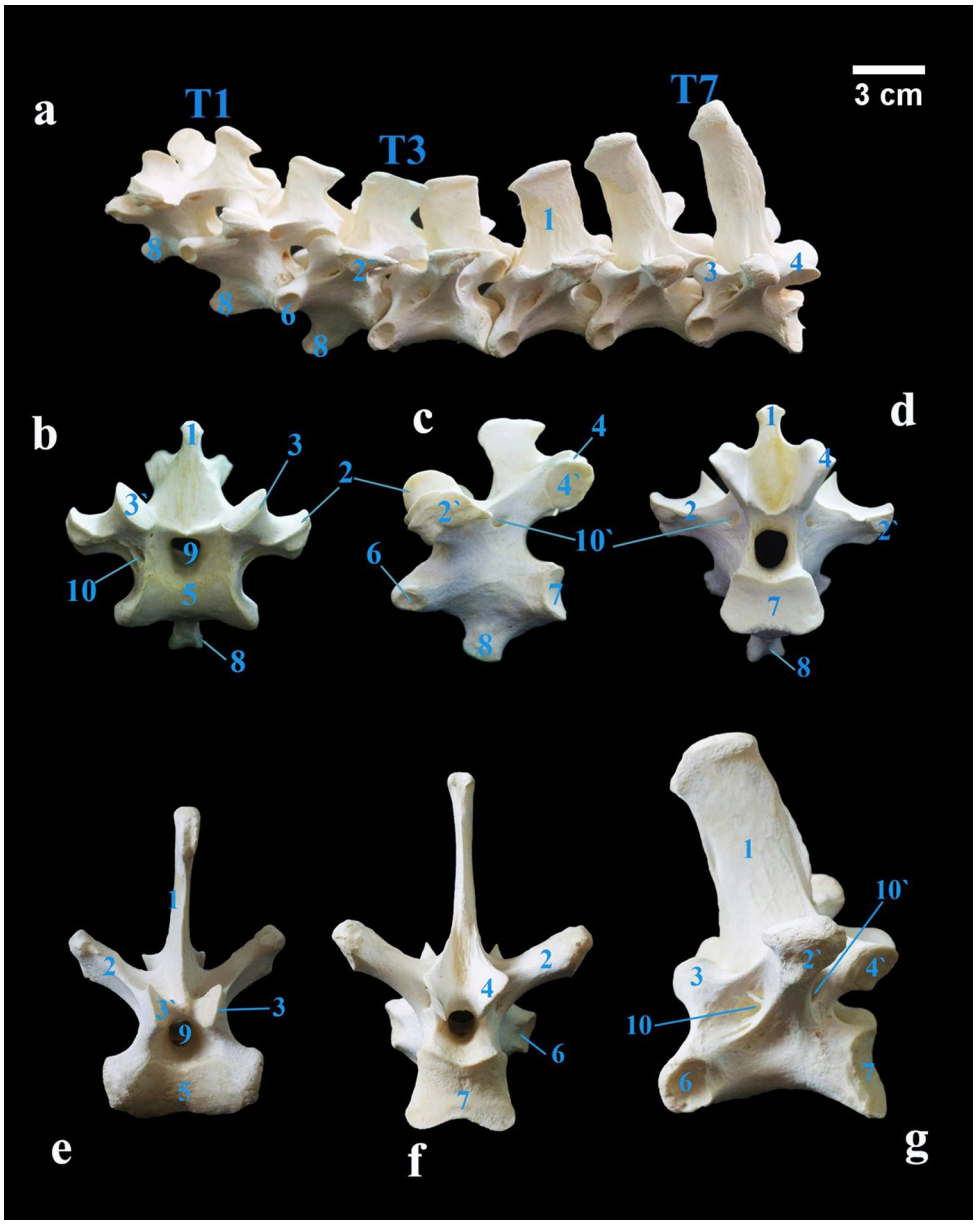


**Fig. 8** **a** Photograph showing the Lateral view of the separated seven thoracic vertebrae of Ostrich, **b**–**d** cranial, lateral and caudal views of T1 respectively, **e**–**g** cranial, caudal and lateral views of T6 respectively. 1 Spinous process. 2 Transverse process. 2' *fovea costalis transversalis*. 3 Cranial articular process. 3' Cranial articular facet. 4 Caudal articular process. 4' Caudal articular facet. 5 Cranial articular surface. 6 *fovea costalis*. 7 Caudal articular surface. 8 Ventral process. 9 Vertebral foramen. 10 Pneumatic foramen (cranial one). 10' *Pneumatic foramen* (caudal one)

slightly till the fifth thoracic vertebrae then decreased in length. The first three thoracic vertebrae had well-developed cranioventrally directed ventral spinous processes (Fig. 8a, c). The body had the costal facet (Fig. 8c) ventrolateral to the cranial articular process. The transverse processes were wide, and plate-like, which increased in width gradually (Fig. 8a) and then increased more at the fourth vertebrae and the processes became to be directed caudodorsal with thick ends (Fig. 8f). Laterally, it carried the transverse costal facet which articulated with the corresponding rib at the tubercular facet (Fig. 8g). The first thoracic vertebra had caudal articular surface (Fig. 8d). The metric data of thoracic vertebrae is shown in (Table 3).

*Synsacrum* (Fig. 9) comprised of fused mass of twenty vertebrae: the last two thoracic, seven lumbar, five sacral, and six caudal vertebrae (Figs. 6b, 9b). On the dorsal surface of the *synsacrum*, *Crista spinosa synsacri* was formed by the fusion of the spinous process of last two thoracic and lumbar vertebrae, also the five sacral vertebrae had four dorsal sacral foramina (Fig. 9a). *Iliosynsacral fissure* was found caudally between the postacetabular ilium and the Spinous processes of caudal vertebrae (Fig. 9a). On the ventral surface of *synsacrum*, *Sulcus ventralis synsacra* was a narrow groove ventrally on the fused bodies of *synsacrum* (Fig. 9b). The *synsacrum* was related caudoventrally to ischium and pubis (Fig. 9c).

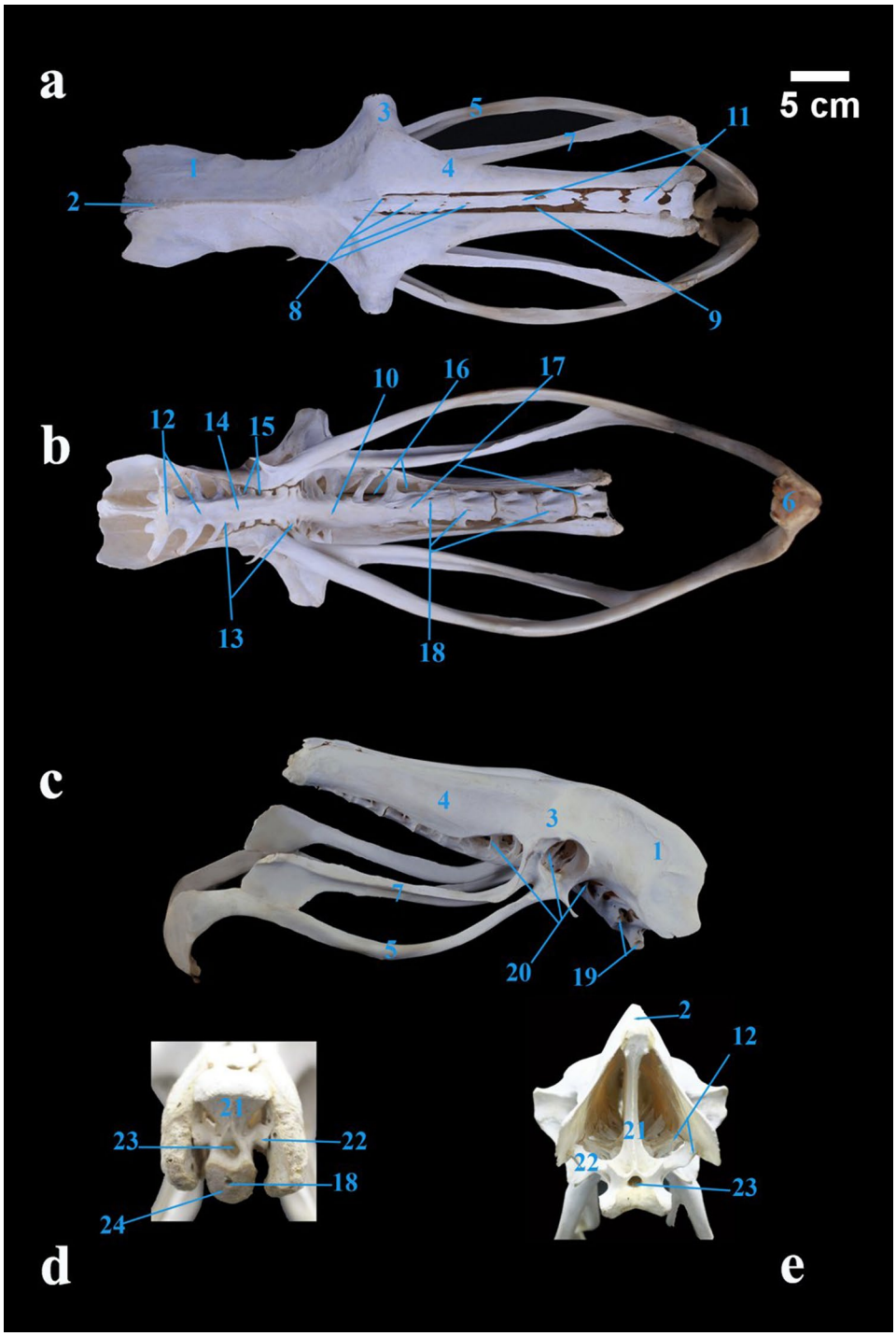


**Fig. 9** **a**–**c** Dorsal, ventral and lateral views of *Synsacrum* and Os coxae of Ostrich. **d**, **e** Caudal and Cranial views of *synsacrum*. 1 Preacetabular ilium. 2 *Crista spinsa synsacri*. 3 Antitrochanter. 4 Postacetabular ilium. 5 Pubis. 6 Symphysis of pubis (apex). 7 Ischium. 8. Dorsal sacral foramina. 9 *Iliosynsacral fissure*. 10 Sacral vertebrae. 11 Spinous processes of caudal vertebrae. 12 Fused Thoracic vertebra 8th and 9th. 13 Fused Lumbar vertebrae. 14 *Sulcus ventralis synsacra*. 15 Ventral foramina of lumbar vertebrae. 16 Intertransversal openings. 17 Ventral surface of Caudal vertebra fused with *synsacrum*. 18 *Pneumatic foramen*. 19 Costal facets. 20 Transverse processes of *synsacrum*. 21 Spinous process. 22 Transverse process. 23 Synsacral canal. 24 Caudal articular surface of *synsacrum*

The Caudal vertebrae (*vertebrae caudales*) of ostrich were fifteen in number, comprising six vertebrae fused with *synsacrum*, in addition to separated, free nine vertebrae, including the pygostyle (Fig. 10a). Most of the caudal vertebrae had prominent *pneumatic foramina* on lateral, dorsal and ventral aspects of their bodies. The spinous processes were double, and they decreased in size caudally. The transverse processes were short and broad, directed caudally which decreased in size in the 13th and 14th caudal vertebrae. The ventral crest was absent. The pygostyle was quadrilateral plate in shape with narrow *lamina pygostyle* (Fig. 10b) dorsally and triangular *basis pygostyle* (Fig. 10c) ventrally.

The thoracic cage of ostrich was formed dorsally by seven separated thoracic vertebrae and two thoracic vertebrae (part of fused synsacrum), laterally; by nine ribs (Fig. 11a), and

**Table 3** Showing the metric data of some selected thoracic and caudal vertebrae of ostrich (*Struthio camelus*)

| | Length (Cm) | Width (Cm) | Height (Cm) |
|---|---|---|---|
| First thoracic vertebra | 4.00 ± 0.28 | 4.00 ± 0.14 | 7.50 ± 0.23 |
| Seventh thoracic vertebra | 4.30 ± 0.34 | 4.80 ± 0.11 | 11.00 ± 0.24 |
| First caudal vertebra | 2.20 ± 0.14 | 2.20 ± 0.08 | 4.50 ± 0.17 |
| Eighth caudal vertebra | 1.20 ± 0.05 | 1.00 ± 0.16 | 1.80 ± 0.08 |
| Pygostyle | 4.00 ± 0.14 | 1.20 ± 0.10 | 2.80 ± 0.17 |

Length was measured from the body ventrally; height was measured from body ventrally to the top of spinous process

cranioventrally; the sternum (Fig. 11f). The Ostrich ribs (*Costae*) were nine pairs in number (Fig. 11a), divided into sternal (true) ribs and asternal (floating) ribs. The sternal ribs extended from the third to the seventh rib, consisting of both vertebral and sternal parts while the rest were asternal floating ribs, consisting of vertebral parts only. Each rib articulated dorsally with its corresponding vertebra while ventrally it articulated with the costal facets of the sternum.

Each rib consisted of a shaft and two extremities: proximal and distal (Fig. 11b). The proximal extremity of the rib was a wide segment consisting of a head (Fig. 11c), neck (Fig. 11d), and tubercle (Fig. 11c), the rib head was craniventral to the tubercle and carried a concave articular facet (Fig. 11d) which articulated with its corresponding costal facet of the thoracic vertebra. The rib tubercle articulated with its corresponding transverse costal facet of the thoracic vertebrae (Fig. 11c). A small pneumatic foramen was noticed between the head and tubercle (Fig. 11b).

The ventral extremity of the sternal rib was thick and carried an articular facet for articulation with the corresponding facets on the sternum. The 8th & 9th floating ribs had thin pointed distal ends (Fig. 11d, e) while those of the 1st and 2nd ribs (Fig. 11c, d) were wide and flat. Each rib had lateral

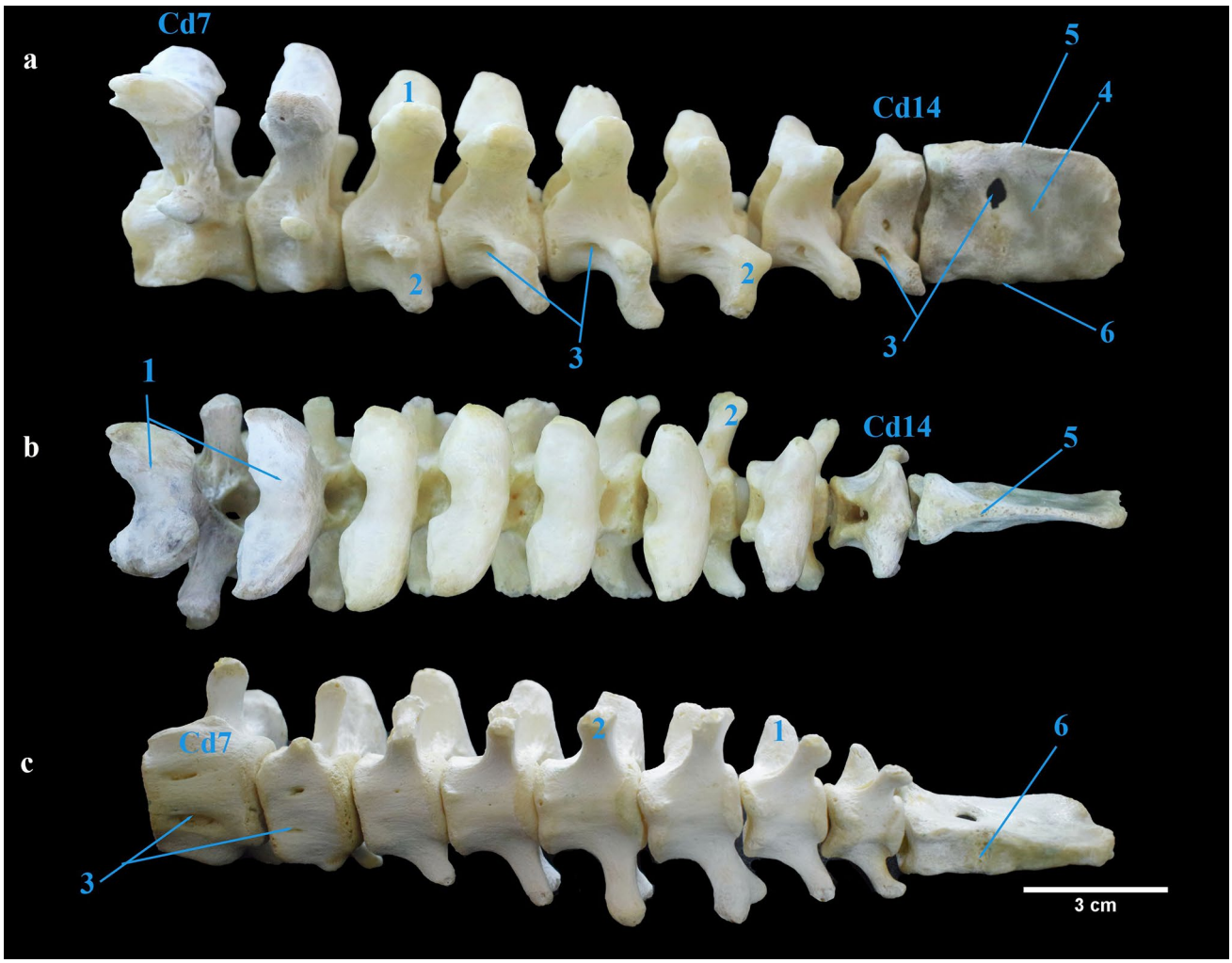


**Fig. 10** **a–c** Lateral, dorsal and ventrolateral views of the free nine caudal vertebrae of Ostrich. 1 Double spinous process. 2 Transverse process. 3 Pneumatic foramen. 4 Pygostyle. 5 Lamina pygostyle. 6 Basis pygostyle. Cd7 7th caudal vertebra. Cd14 14th caudal vertebra

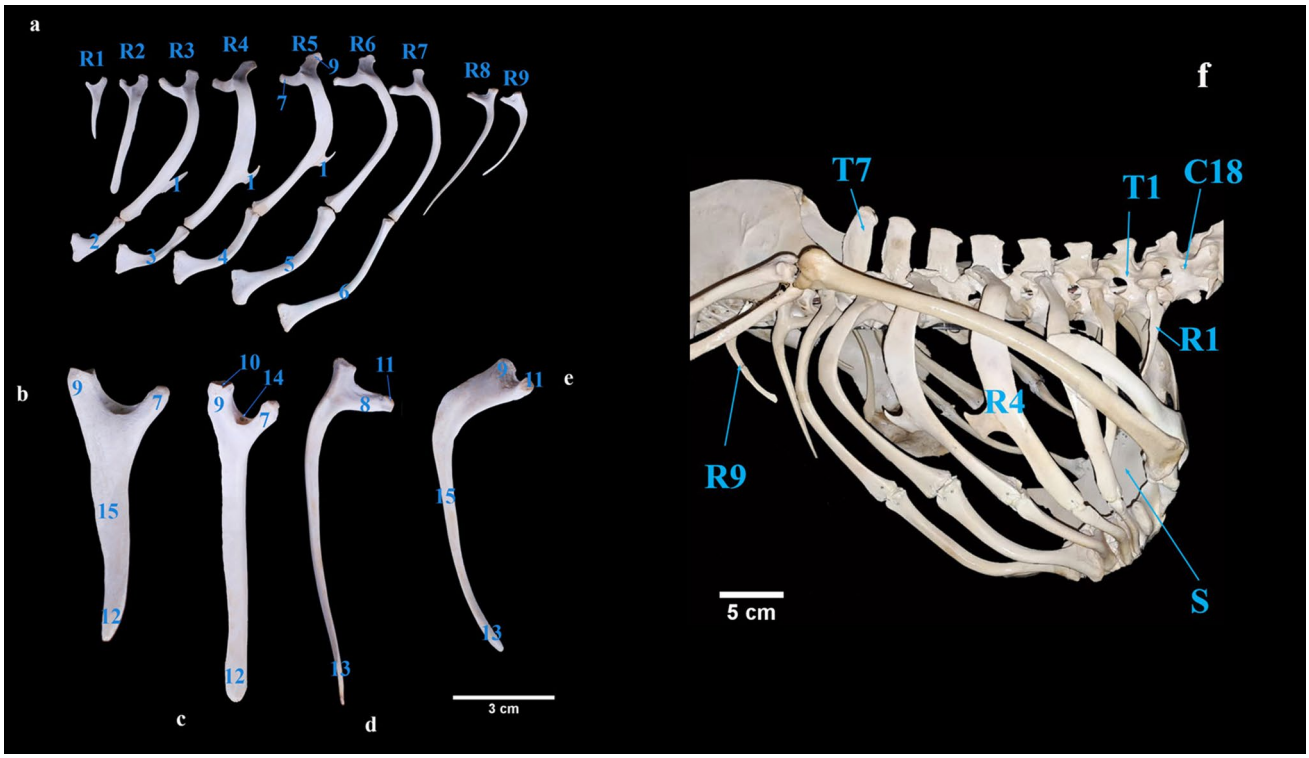


**Fig. 11** **a** The lateral view of the ribs of Ostrich (*Struthio camelus*), **b–e** Medial view of floating ribs 1st, 2nd, 8th & 9th respectively. R1 First rib. R2 Second rib. R3 Third rib. R4 Fourth rib. R5 Fifth rib. R6 Sixth rib. R7 Seventh rib. R8 Eighth rib. R9 Ninth rib. 1 Uncinate process. 2 Sternal part of R3. 3 Sternal part of R4. 4 Sternal part of R5. 5 Sternal part of R6. 6 Sternal part of R7. 7 Head. 8 Neck. 9 Tubercle. 10 Tubercular facet. 11 Articular facet. 12 Distal extremity (broad end). 13 Distal extremity (pointed end). 14 Pneumatic foramen. 15 Shaft. **f** The thoracic cage of ostrich mounted in situ. C18 Eighteenth cervical vertebra. T1 First thoracic vertebra. T7 Seventh thoracic vertebra. R1 First rib. R4 Fourth rib. R9 Ninth rib. S Sternum

**Table 4** Showing the metric data of the ribs of ostrich (*Struthio camelus*)

| | Length (from the tubercle to the distal end of the rib) (cm) |
|---|---|
| First rib | 8.00 ± 0.25 |
| Fifth rib | 40.00 ± 0.31 |
| Seventh rib | 41.00 ± 0.37 |
| Eighth rib | 19.00 ± 0.34 |

convex, and medial concave surfaces, in addition to a thin cranial border and a slightly thick caudal one. The vertebral parts of the third, fourth and fifth ribs carried small uncinate process on their caudal borders (Fig. 11a) directed dorsally. The metric data of ribs is shown in (Table 4).

The sternum of ostrich was a broad quadrilateral extensive bone found in the cranioventral aspect of the thorax. It lacked the keel bone. Anatomically the term meta sternum was applied to the caudal region of the sternum while costal sternum was applied to the area designated for articulation with the ribs. The caudal border of the sternum appeared solid compact area and non-fenestrated. The sternum had two surfaces (dorsal and ventral), two extremities (cranial and caudal), and four borders (cranial, caudal, and two lateral). The dorsal surface of the sternum formed a quadrilateral expanded plate, strongly concave (Fig. 12a). The cranial part of the dorsal surface was wider than the meta sternum area. The ventral surface was convex and rough for muscular attachment (Fig. 12). The cranial border was convex, and broader than the caudal one (Fig. 12a). The cranial extremity carried two *coracoid articular sulci* (Fig. 12c). Bilaterally, it bulged to form two eminences known as craniolateral processes which had several *pneumatic foramina* dorsally (Fig. 12a). The caudal border was sharply convex, and it formed a xiphoid process at its middle and the long caudally directed thoracic processes (Fig. 12b). The lateral (costal) border bore five pairs of costal articular facets (Fig. 12a, e) with wide excavated Interarticular areas in between. The metric data of sternum is shown in (Table 5).

## Discussion

The ostrich skull was mostly pneumatic as reported earlier (Moselhy et al. 2018). The splanchnocranium included the ethmoid bone in our study, while another literature showed

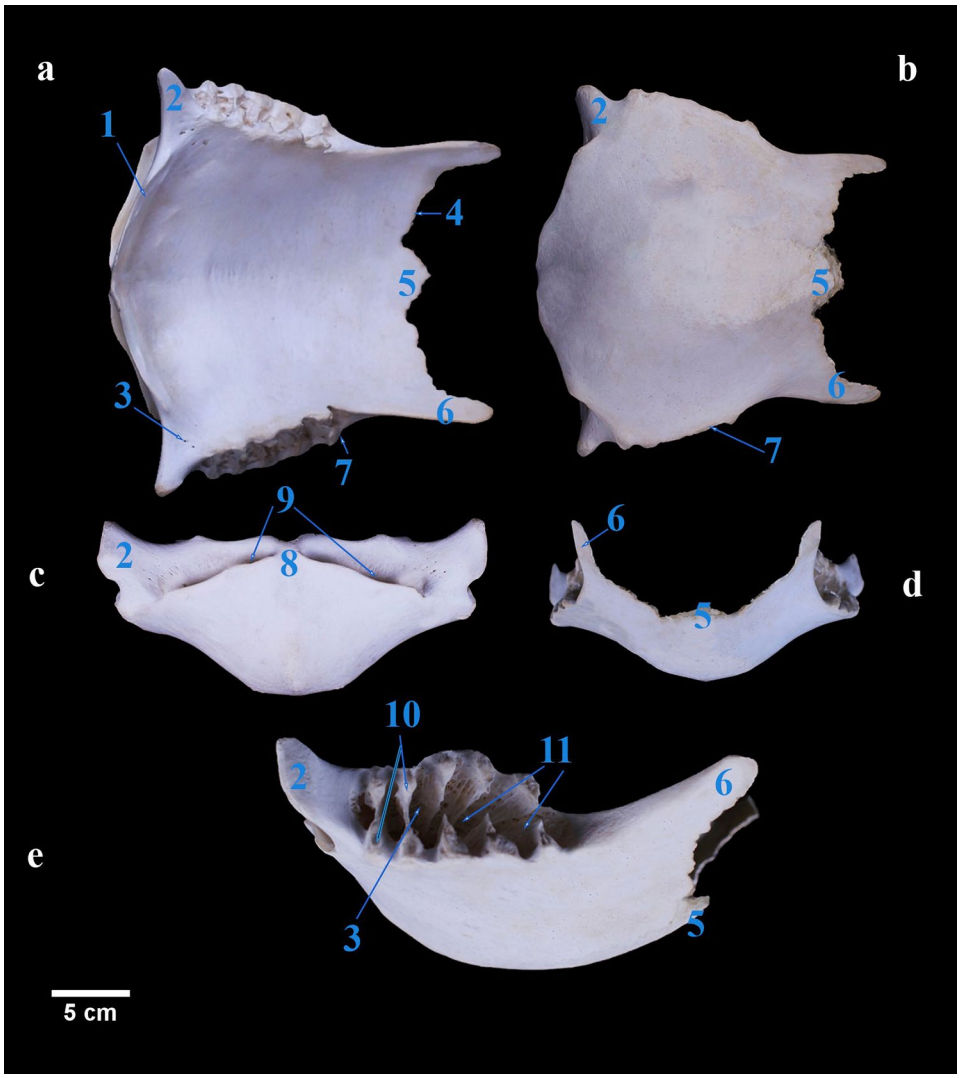


**Fig. 12** **a–e** The dorsal, ventral, cranial and caudal views of the ostrich sternum (*Struthio camelus*) respectively. 1 Cranial border. 2 Craniolateral process. 3 Pneumatic foramen. 4 Caudal border. 5 Xiphoid process (caudal extremity). 6 Thoracic process. 7 Lateral border. 8 Cranial extremity. 9 Coracoid articular sulcus. 10 Costal articular facets. 11 Interarticular area

**Table 5** Showing the metric data of the sternum of ostrich (*Struthio camelus*)

| | Length (cm) | Width (cm) |
|---|---|---|
| Sternum | 22.50 ± 0.29 (from the craniolateral process to xiphoid process) | 24.00 ± 0.23 (Cranially)<br>22.00 ± 0.40 (at the middle)<br>15.00 ± 0.29 (caudally) |

that the ethmoid shared both splanchnocranium and neurocranium (Kumar and Singh 2014). Similar to Emu the occipital bone was composed of three bones: the basioccipital, exoccipital, and supraoccipital bones (Kumar and Singh 2014). In ostrich the supraoccipital bone carried a sagittal nuchal crest which was in agreement with (Moselhy et al. 2018). In addition, the present study showed the arched transverse nuchal crest as described in chicken (Tahon et al. 2013), (Baumel 1993). Conversely, it had a median external occipital protuberance in emu (Kumar and Singh 2014) and in ostrich (Moselhy et al. 2018). The exoccipital bones were paired bones with large protruded paroccipital processes resembling previous studies (Kumar and Singh 2014), (Moselhy et al. 2018).

The present study revealed that the Sphenoid bone was consisted of basisphenoid caudally, parasphenoid rostrally and laterosphenoid laterally (Baumel 1993). Per-contra, in ostrich the sphenoid bone was divided into caudal basisphenoid and rostral presphenoid parts (Moselhy et al. 2018). However, the presphenoidal bone was absent in ostrich (Pop and Pentea 2007).

The current study stated that the Frontal bone had lacrimal, postorbital processes and the orbital wing of the frontal bone. Contradictory, the frontal possessed frontal, orbital

and nasal processes in emu (Kumar and Singh 2014). The present study stated that the squamosal bone had processus zygomaticus and fossa temporalis, and the ossa otica was articulated with the processus oticus of quadrate bone, simulating findings in some birds (Baumel 1993). We added that *Fossa glandulae nasalis* was a depression on the dorsal aspect of the supraorbital margin that was occupied by the salt gland.

The ethmoid bone was consisted of mesethmoidal and ectoethmoidal bones, that was similar to the observations in chicken (Tahon et al. 2013), in birds (Baumel 1993) and in grey heron (Bavdek et al. 2017), in addition to the lamina dorsalis of mesethmoidal bone simulating previous findings (Baumel 1993). Conversely, the ethmoid bone was consisted of horizontal plate and perpendicular plates (Kumar and Singh 2014).

The vomer body fused caudally to the presphenoid bone as described in chicken (Tahon et al. 2013). Regarding the present study the interorbital septum was formed from the orbital wing of frontal bone, mesethmoidal and laterosphenoid bones, also the interorbital septum has a single optic foramen. However, in emu the interorbital septum was formed of the orbital wings of presphenoid, a medial thin bony plate, and the vertical plate of the ethmoid bone (Kumar and Singh 2014). In the present study the ectoethmoidal bone formed the rostral wall of the orbit rostrally to separate it from the nasal cavity (Baumel 1993). On the other hand the ectoethmoidal bone entered in the formation of the interorbital septum (Bavdek et al. 2017).

The nasal bone had frontal, lateral nasal, and Premaxillary processes, in contrary, the nasal bone had frontal process, premaxillary process and maxillary process in chicken (Tahon et al. 2013). In present study, the lacrimal bones were wide comma shaped bones forming the rostral boundary of the orbit, per-contra in owl, the lacrimal bone was a large triangular bone (Sary and Ibrahium 2022). The jugal process of lacrimal bone was bifid caudoventral to join the jugal bone in grey heron (Bavdek et al. 2017) similar to our findings.

In our study, premaxillary bones had frontal and maxillary processes only but it had also palatine processes in previous study (Moselhy et al. 2018). *Rostrum maxillae* had numerous Neurovascular foramina similar to previous reports in birds (Baumel 1993).

We were convinced that the maxillary bones had premaxillary and jugal processes, however in chicken, the maxillary bone had; palatine, jugal, premaxillary and nasal processes (Tahon et al. 2013). The jugal arch was formed of the fused jugal process of maxillary bone, jugal and quadratojugal bones, resemblance previous reports (Kumar and Singh 2014) and (Moselhy et al. 2018).

Palatine bones were quadrilateral plates constituting the bony roof of pharynx, while in chicken, they were rod-like bones parallel to each other (Tahon et al. 2013). The mandibular process of quadrate was well developed carrying caudal, lateral and medial condyles as reported in previous report (Baumel 1993).

The sclerotic ring was a ring of small overlapping bony plates within the eye sclera, in resemblance to that described in birds (Kaiser 2010), (Olsen and Joseph 2011). The Mandible was V-shaped with slightly curved right and left mandibular rami fusing rostrally to form the mandibular symphysis, were also mentioned in cattle egret (Rezk 2015), brown wood owl (Choudhary et al. 2021), birds (Rana et al. 2020), and ostrich and emu (Crole and Soley 2017). The mandible was constituted of seven bones, resemblaning earlier studies (Rezk 2015), (Rana et al. 2020). We revealed that Mandibular bones were fused to each other in the adult by ossification except the suture between angular and supra-angular is not completely ossified.

The hyoid apparatus was comprised of three parts: basihyale, urohyale, and Cornu branchiale, on the contrary, the urohyal bone was absent in woodpeckers (Apostolaki et al. 2015). However, the hyoid apparatus had additionally Os paraglossale in chicken (Tahon et al. 2013) and in cattle egret (Rezk 2015). Our study described that hyoid ramus in ostrich consisted of a proximal bony part *Ceratobranchiale* and slightly curved distal cartilaginous process called the *Epibranchiale*.

The vertebral column comprised 54 vertebrae, in accordance with previous study in ostrich (Deeming 1999). The Cervical column was composed of 18 vertebrae, per-contra, they were 17 in number in ostrich (Apostolaki et al. 2015) and emu (Pop and Pentea 2007), (Kumar and Singh 2014), However, they were 14 cervical vertebrae in chicken (Tahon et al. 2013), and 25 vertebrae in swans (Dyce et al. 2009). The atlas body occupied the Condyloid fossa on its cranial surface for lodging the single occipital condyle of the cranium forming the atlantooccipital joint, in resemblance to previous study in birds (Dyce et al. 2009). The Axis had protruded dens with a rounded tip, per-contra it was triangular-shaped with a blunt tip in emu (Kumar and Singh 2014). The costal processes were pointed spines, directed caudally on the lateral aspect of cervical vertebrae similar to reports in birds (Baumel 1993). We added that several *pneumatic foramina* were found in the cervical vertebrae, also, the transverse foramen was found in all the cervical vertebrae except atlas.

Thoracic vertebrae were nine in number comprising the first seven separated vertebrae and the last two thoracic vertebrae were fused with the *synsacrum*, as also described in emu (Rajalakshmi et al. 2020). Per-contra the thoracic vertebrae were ten in number in emu (Kumar and Singh 2014). Our study detected that ostrich did not contain a notarium as other previous reports (Wagner et al. 2001). We added that all thoracic vertebrae had pneumatic foramina both cranially and caudally.

In our study, *Synsacrum* comprised 20 vertebrae, while they were 15 in number in ostrich (Apostolaki et al. 2015). *Synsacrum* comprised the fused last two thoracic, seven lumbar, five sacral, and six caudal vertebrae. However, the lumbosacral mass was formed by the last two fused thoracic, six lumbar, ten sacral, and first coccygeal vertebrae in Emu (Rajalakshmi et al. 2020). The Caudal vertebrae were 15 in number, comprising six vertebrae fused with *synsacrum*, in addition to separated, free 9 vertebrae, including the pygostyle, while they were seven free caudal vertebrae in ostrich (Apostolaki et al. 2015). However, there were free five coccygeal vertebrae in emu (Rajalakshmi et al. 2020). Most of the caudal vertebrae have prominent *pneumatic* similar to descriptions in ostrich (Wedel and Taylor 2013), also we described that most of the caudal vertebrae had prominent *Pneumatic foramina* on lateral, dorsal and ventral aspects of their bodies.

The ribs were nine pairs in number, divided into sternal ribs and asternal ribs that was concurred with earlier reports in ostrich (Wagner et al. 2001), (Brett and Hopkins 1991) and emu (Kumar and Singh 2014). The floating ribs were the 1st, 2nd, 8th and 9th in our study, while the 1st, 2nd, 3rd, 8th and 9th were floating ribs and the rest were complete ribs in emu (Kumar and Singh 2014).

The sternum lacked the keel bone which was accordance to finding in ostrich and emu (Feneck et al. 2021). The sternum was quadrilateral in shape similar to previous observations in ostrich (Predoi et al. 2009), spot billed pelican (Sathyamoorthy et al. 2012) and green winged macaw (Sreeranjini et al. 2015) and was in contrast to the rectangular sternum in duck (Jayachitra et al. 2015). The sternum lateral borders had five pairs of costal facets with wide excavated interarticular areas in between, similar to earlier observations in emu (Mehta et al. 2017) but was contrary to observations that the costal facets were six in ostrich (Predoi et al. 2009) and in green winged macaw (Sreeranjini et al. 2015). However, the sternum costal facets were four in number in chicken (Tahon et al. 2013).

## Conclusion

For the anatomical descriptions, the Ostrich Vertebral formula was C18 T9 L7 S5 Cd 6 + 9, and the total number of vertebrae was 54. The vertebral column was highly pneumatic including the cervical, thoracic, and caudal vertebrae**.** The ribs were nine pairs in number. The sternum was a broad quadrilateral extensive bone but lacking the keel bone. Both the ribs and sternum showed *pneumatic foramina*.

In the frontal bone, *Fossa glandulae nasalis* was a depression on the dorsal aspect of the supraorbital margin that was occupied by the salt gland. In the hyoid apparatus, *Cornu branchiale* consisted of a proximal bony part *Ceratobranchiale* and distal cartilaginous process *Epibranchiale*. The Os mesethmoidale formed most of the interorbital septum rostrally, it formed lamina dorsalis perpendicular to interorbital septum. The sclerotic ring was a ring of small bony plates within the eye sclera.

Morphometrically, the cranium length was 20.00 ± 1.09 cm. The mandible was 16.50 ± 0.28 cm in length. The atlas length was 0.40 ± 0.05 cm, the axis length was 3.20 ± 0.11 cm then increased gradually till the 18th cervical vertebra with an average length of 6.34 ± 0.22 cm. The maximum height of thoracic vertebrae reached 11.00 ± 0.24 cm while that of caudal vertebrae was 4.50 ± 0.17 cm. The length of 1st thoracic vertebra was 4.00 ± 0.28 cm while the 1st caudal was 2.20 ± 0.14 cm. The pygostyle length was 4.00 ± 0.14 cm. The longest rib was the seventh rib, which reached 41.00 ± 0.37 cm and the shortest rib was the first one which measured 8.00 ± 0.25 cm. The sternum length was 22.50 ± 0.29 cm.

## Materials and methods

The present study was conducted on axial skeleton of 7 male ostriches aged from 1 to 3 years with an average weight of 120.00 kg. Most of them were collected either from recently died birds (accidental death) or after slaughter for human consumption. They were obtained from Abu Rifai Ostrich Farm in the European countryside at Cairo-Alexandria Desert Road in Egypt.

*Specimen preparation*: The obtained carcasses were dissected manually to remove skin, muscles, viscera with the aid of ordinary dissecting tools as dissecting forceps, scissors, and scalpels. A metal wire was inserted into the neural canal, foramen magnum to evacuate the brain and spinal cord and for stabilizing the vertebrae.

*Cleaning the bones*: The maceration process was enhanced by boiling the specimens for 2 h in 5% potassium hydroxide (KOH) (Tahon et al. 2013) and (Kassem et al. 2023), then left for 5 days in the open air after cleaning. Only the skull was macerated by soaking it in hot water with 5% sodium bicarbonate for 30 min (Sary and Ibrahium 2022) and then washed with water.

*Bleaching process*: The bleaching of bones was obtained by soaking them in 5% hydrogen peroxide for 3 days (Sullivan and Romney 1999) for the vertebral column but only for 30 min for the skull. The bones were photographed using a cannon digital camera, 16.1 MP, 4x. The nomenclature was according to *Nomina Anatomica Avium* (Baumel 1993).

*For metric study*: Measurement of 3 ostrich bones (length, width and height) in this study were performed using a digital Vernier caliper. Statistical analysis was described as mean value ± standard error using Microsoft excel 2010.

**Acknowledgements** We thank Cairo University for their help to complete our work.

**Author contributions** MAMK performed the protocol of anatomical study of ostrich bones and analyzed the data. RRT contributed substantially to conceptualizing work, interpretation of the data, drafting the work, and discussion of the results. MAEA designed the protocol, gathered the work plan, drafted the work, and reviewed the manuscript. All authors contributed to the revision of the manuscript. All authors approved the submitted version of the manuscript.

**Funding** Open access funding provided by The Science, Technology & Innovation Funding Authority (STDF) in cooperation with The Egyptian Knowledge Bank (EKB).

**Data availability** The datasets are available from the corresponding author on reasonable request. The whole skeleton of ostrich was mounted in our museum of the Department of Anatomy and Embryology, Faculty of Veterinary Medicine, Cairo University.

## Declarations

**Conflict of interest** The authors declare no competing interest.

**Ethical approval and consent to participate** The study was conducted by the international ethical standards set by the institutional animal care and use committee (Vet CU 2009 2022532).



## References

Apostolaki NE, Rayfield EJ, Barrett PM (2015) Osteological and soft-tissue evidence for pneumatization in the cervical column of the ostrich (*Struthio camelus*) and observations on the vertebral columns of non-volant, semi-volant and semi-aquatic birds. PLoS ONE 10(12):e0143834

Baumel JJ (1993) Handbook of avian anatomy: nomina anatomica avium. Publications of the Nuttall Ornithological Club, USA, p 23

Bavdek SV, Golob Z, Janžekovič F, Rutland CS, Kubale V (2017) Skull of the grey heron (*Ardea cinerea*): detailed investigation of the orbital region. Anat Histol Embryol 46(6):552–557

Brett A, Hopkins M (1991) Anatomy of ostriches, emus and rheas. The Ratite Encyclopedia. 1st edn. Columbia, USA, pp. 32–36

Choudhary O, Priyanka P, Arya R (2021) Morphometric and radiographic characteristics of the skull in crested serpent eagle (*Spilornis cheela*) and brown wood owl (*Strix leptogrammica*). Indian J Anim Res 55(4):426–432

Crole MR, Soley JT (2017) Bony pits in the ostrich (*Struthio camelus*) and emu (*Dromaius novaehollandiae*) bill tip. Anat Rec 300(9):1705–1715

Deeming DC (1999) The ostrich: biology, production and health. CAB International

Dyce KM, Sack WO, Wensing CJG (2009) Textbook of veterinary anatomy-E-Book. Elsevier Health Sciences, Amsterdam

Feneck EM, Bickley SR, Logan MP (2021) Embryonic development of the avian sternum and its morphological adaptations for optimizing locomotion. Diversity 13(10):481

Jayachitra S, Balasundaram K, Paramasivan S (2015) Comparative gross anatomical studies on the sternum of emu, turkey and duck. J Anim Res 5(2):385

Kaiser GW (2010) The inner bird: anatomy and evolution. UBC Press, Vancouver

Kassem MAM, Tahon RR, Khalil KM, El-Ayat MA (2023) Morphometric studies on the appendicular bony skeleton of the ostriches (*Struthio camelus*). BMC Vet Res 19(1):109

Kumar P, Singh G (2014) Gross anatomy of axial skeleton in Emu (*Dromaius novaehollandiae*). Indian J Vet Anat 26(2):87–91

Kummrow MS (2015) Ratites or struthioniformes: struthiones, rheae, cassuarii, apteryges (ostriches, rheas, emus, cassowaries, and kiwis), and tinamiformes (tinamous). Fowler's Zoo Wild Anim Med 8:75

Mehta S, Rupam S, Singh K (2017) Gross morphometric studies on sternum and ribs of emu (*Dromaius novaehollandiae*). Vet Sci Res J 8(1/2):47–49

Mikhailov KE, Zelenkov N (2020) The late Cenozoic history of the ostriches (Aves: Struthionidae), as revealed by fossil eggshell and bone remains. Earth Sci Rev 208:103270

Moselhy AA, Mohamed SKA, El-Ghazali HM (2018) Anatomical features of bones and bony cavities of the ostrich skull (*Struthio camelus*). Int J Anat Res 6(2.3):5390–5398

Olsen P, Joseph L (2011) Stray feathers: reflections on the structure, behaviour and evolution of birds. Csiro Publishing, Clayton

Pop C, Pentea M (2007) The osteological features of the skeleton in ostrich (struthio camelus). Lucrări Stiin$^3$ifice Medicinã Veterinarã, Timisoara. Calea Aradului 40:561–568

Predoi G, Belu C, Dumitrescu I, Georgescu B, Seicaru A, Rosu P, Carmen B, Dumitrescu F (2009) Comparative researches regarding the sternum in ostrich (*Struthio camelus*) and Nandu (*Rhea americana*). Lucrari Sci Med Vet 42:342–346

Rajalakshmi K, Sridevi P, Siva Kumar M (2020) Gross anatomical studies on thoracic, Synsacrum, coccygeal vertebrae and ribs of emu (Dromaius novaehollandiae). Pharma Innovation J 9(1):211–215

Rana J, Patel SK, Banubakode S, Charjan R (2020) Comparative gross morphological studies on the lower jaw (Mandible) of cattle egret (Bubulcus ibis), jungle babbler (Turdoides striata), yellow-footed green pigeon (Treron phoenicoptera), barn owl (Tyto alba) and shikra (Accipiter badius). Int J Livestock Res 10(10):105–110

Rezk HM (2015) Anatomical investigation on the axial skeleton of the cattle egret *Bubulcus ibis*. Assiut Vet Med J 61(145):12–21

Sary R, Ibrahium A (2022) Computerized tomography, radiological and morphological features on the skull of Egyptian owl (*Bubo ascalaphus*). Adv Anim Vet Sci 10(8):1810–1817

Sathyamoorthy O, Thirumurugan R, Senthil Kumar K, Jayathangaraj M (2012) Gross anatomical studies on the sternum and clavicle of spot-billed pelican (*Pelecanus philippensis*). Tamilnadu J Vet Anim Sci 8(3):166–170

Sreeranjini A, Ashok N, Indu V, Lucy K, Maya S, Chungath J (2015) Gross anatomical features of the sternum of green-winged macaw (*Ara chloroptera*). Indian J Anim Res 49(6):860–862

Sullivan L, Romney C (1999) Cleaning and preserving animal skulls. The University of Arizona Cooperative Extension, AZ1144, 1999

Tahon R, Ragab S, Abdel Hamid M, Rezk H (2013) Some anatomical studies on the skeleton of chickens. Anatomy and Embryology, Faculty of Veterinary Medicine, Cairo University. Ph. D. Thesis

Wagner W, Kirberger R, Groenewald H (2001) Radiographic anatomy of the thoraco-abdominal cavity of the ostrich (*Struthio camelus*). J S Afr Vet Assoc 72(4):203–208

Wedel MJ, Taylor MP (2013) Caudal pneumaticity and pneumatic hiatuses in the sauropod dinosaurs Giraffatitan and Apatosaurus. PLoS ONE 8(10):e78213